Indian Ocean Dipole and Rainfall drive a Moran Effect in East Africa Malaria transmission

Luis Fernando Chaves[1,2 *], Akiko Satake[1], Masahiro Hashizume[3], and Noboru Minakawa[3]

[1]Graduate School of Environmental Sciences and Global Center of Excellence program on Integrated Field Environmental Science, Hokkaido University, Sapporo, Japan

[2] Programa de Investigación en Enfermedades Tropicales, Escuela de Medicina Veterinaria, Universidad Nacional, Heredia, Costa Rica

[3]Institute of Tropical Medicine (NEKKEN) and Global Center of Excellence program on Tropical and Emergent Infectious Diseases, Nagasaki University, Nagasaki, Japan

Short title: **Climate and Moran effect in malaria**

Footnote

The authors declare no competing interests and that funding agencies had no role on study design.

Funding This work was funded by Japan Society for the Promotion of Science and a Nagasaki University Cooperative Research Grant.

*corresponding author. Address: Graduate School of Environmental Sciences, Hokkaido University, Room A701 5-chome, Kita 10-jo Nishi, Kita-ku, Sapporo 060-0810, Hokkaido, Japan. Phone: +81-11-706-2267. Fax: +81-11-706-4954. Email: lchaves@ees.hokudai.ac.jp

Category: **Major Article**

197 Words in the abstract

3343 words (including: 26 References + Figure Legends)

6 Figures + 1 Table

Supplementary data:

Detailed methods

Abstract

Background: Patterns of concerted fluctuation in populations, synchrony, can reveal impacts of climatic variability on disease dynamics. Here, we examined whether malaria transmission has been synchronous in an area with a common rainfall regime and sensitive to the Indian Ocean Dipole (IOD), a global climatic phenomenon affecting weather patterns in East Africa.

Methods: We studied malaria synchrony in five fifteen year long (1984-1999) monthly time series that encompass an altitudinal gradient, ~1000m to 2000m, along Lake Victoria Basin. We quantified the association patterns between rainfall and malaria time series at different altitudes and across the altitudinal gradient encompassed by the study locations.

Results: We found a positive seasonal association of rainfall with malaria, which decreased with altitude. By contrast, IOD and interannual rainfall impacts on interannual disease cycles increased with altitude. Our analysis revealed a non-decaying synchrony of similar magnitude in both malaria and rainfall, as expected under a Moran effect, supporting a role for climatic variability on malaria epidemics frequency, which might reflect rainfall mediated changes in mosquito abundance.

Conclusion: Synchronous malaria epidemics call for the integration of knowledge on the forcing of malaria transmission by environmental variability to develop robust malaria control and elimination programs.

Key-words: Synchrony, Climate Change, Indian Ocean Dipole, *Anopheles*, *Plasmodium*, Time Series

Synchrony, the degree of concerted fluctuations among populations in a region, is a key parameter to understand impacts of climatic trends and variability on population dynamics [1]. For infectious diseases, synchrony has become especially important because its estimation offers a mean to test hypothesis regarding the importance of exogenous epidemic drivers. In a relatively homogenous environment, a synchrony decay with distance implies that impacts of climatic trends and variability, if any, are marginal when compared with regulatory factors related to population processes, e.g., immunity in diseases, and independent of the changing environment [2]. By contrast, a non-decaying synchrony, of magnitude slightly larger, or similar, to that of the environment, will support a Moran effect, where transmission patterns in a region could be similar by a common mechanism of action for the exogenous, often climatic, forcing [3]. As originally defined, the Moran effect arises by the emerging synchronization of autoregressive dynamics of time series by the impact of common sources of exogenous forcing, i.e., the autonomous (or endogenous) dynamics of a population get tuned to that of external factors influencing the dynamics of populations living under a similar (or correlated) environment [2].

Vector-borne diseases, such as malaria, are excellent model systems to study synchrony and test Moran effects. For example, Moran effects are expected in malaria because of the monotonic relationship between vector abundance and transmission [4], and between vectors and rainfall [5]. Lake Victoria basin (LVB) is a unique setting to study exogenous forcing in malaria transmission because of three main reasons: (i) it encompasses an altitudinal gradient, which is also a gradient of malaria endemicity [6, 7]; (ii) it has relatively homogeneous rainfall patterns [8]; (iii) rainfall and malaria are impacted by global climatic phenomena, especially the Indian Ocean Dipole, an irregular oscillation of sea-surface temperatures in which the western Indian Ocean becomes alternately warmer and then colder than the eastern part of the ocean [9, 10].

Here, we studied malaria synchrony in five fifteen year long (1984-1999) monthly time series (Fig. 1A) from Lake Victoria basin, West Kenya (Fig. 2). We also studied rainfall time series (Fig. 1B) synchrony to test the condition of environmental autocorrelation necessary for a Moran effect. We used the dipole mode index, DMI, (Fig. 1C) as an IOD index [11] to quantify its role as interannual driver of malaria and rainfall dynamics. We found that both rainfall and malaria had a non-decaying synchrony with distance, and that malaria synchrony was slightly larger than

rainfall synchrony, as expected under a Moran effect. A more detailed time scale analysis of synchrony showed that seasonal cycles in malaria transmission were led by two month lagged changes in rainfall, with decreasing intensity as a function of altitude. By contrast, interannual cycles in the disease were driven by IOD, with an increasing intensity with altitude. These patterns could be related to the population dynamics of *Anopheles* mosquitoes, whose abundance is likely driven by rainfall patterns in the region [5, 12]. Finally, our results clearly show that patterns of climatic variability have a strong signature in malaria transmission among vulnerable populations, and are, therefore, a necessary input for a strong malaria control/elimination framework.

Materials and Methods

Data Malaria and rainfall data spanned from January 1985 to December 1999. The five malaria time series were monthly counts of inpatients admitted into the hospitals because of high fever and other clinical malaria symptoms. In Kericho, all malaria cases were confirmed by blood slide examination [13]. In the other four sites (Maseno, Kendu Bay, Kisii and Kapsabet) we collected the data from books with malaria diagnosed inpatient records. Unfortunately, these books did not indicate whether all recorded malaria cases were confirmed by blood slide examination. However, we were informed by staff members from each hospital that cases were often confirmed by blood slide examination. We restricted our samples to this kind of malaria infections, i.e., inpatient admissions, in order to make a sound statistical analysis at the price of using data that likely underestimate the total number of malaria infections [14]. Rainfall data were obtained from the Kenyan Meteorological service. We use rainfall records from some of the same locations of the malaria time series and a location midway between the two lowest altitude sites (Fig. 2). Specifically, we employ meteorological records from Kisumu as proxy inputs for Kendu Bay and Maseno, localities for which we were unable to find relatively complete records through the Kenyan Meteorological services and other meteorological data repositories. We chose Kisumu because of the lack of missing observations during the study period, and by the similar rainfall patterns to Kendu Bay and Maseno according to meteorological models [8].

Statistical Analysis To estimate synchrony in the time series first we removed non-stationary trends [15] in the malaria time series(Fig. 1D) using three standard procedures: local polynomial regression fitting (Loess) [15], singular spectrum analysis (SSA) [16] and the empirical mode decomposition (EMD) [17]. These methods have different assumptions and outcomes, Loess extracts (non)linear trends (Fig. 1E), while SSA (Fig. 1F) and EMD decompose signals into different oscillatory (Fig. 1G, 1H and 1I) and non-cyclical components. In SSA the trends are extracted by examining the variability of the largest eigenvalue from an autocovariance matrix, while EMD decomposes a time series by building oscillatory signals, Intrinsic Mode Functions (IMF), that are repeatedly subtracted from the time series. We employed these different methods to ensure robustness in the inferences from subsequent analyses. The lack of non-stationary trends in rainfall made unnecessary the treatment with Loess and SSA. However, we decomposed rainfall data using EMD to perform frequency specific association analysis (Fig. 3). Second, we estimated the synchrony, r_0, i.e., cross correlation at lag 0, of rainfall and detrended malaria time series, using both linear regression [2] and spline correlogram on high frequency filtered, detrended time series [18]. Third, we studied the association between rainfall and DMI with malaria along the altitudinal gradient of our study locations using cross correlation functions [15]. Further details about the data and methods are presented in the Supplementary Data.

Results

Estimates for malaria regional synchrony (Table 1) were similar using SSA, Loess (Fig. 4A) and EMD (Fig. 4B) detrended time series. Malaria time series synchronicity was observed across the 2-dimensional distance, and altitude, gradients, with all series in phase and with their maximum correlation observed at lag 0 (Fig. 4C), with minimum correlations well above 0.3 at lag 0 in the EMD detrended malaria data (Fig 4B, 4C, Table 1). For rainfall, synchrony estimates from the raw time series (Fig. 4D) and EMD (Fig. 4E) were very similar across the range of distances and altitudes studied (Fig. 4F). To estimate the smoothed correlogram of malaria (Fig. 4B) and rainfall (Fig. 4E) we employed only the EMD detrended time series since this procedure also allowed to filter out high frequency components in the time series, which can artificially increase time series synchrony by the emerging correlation expected from high frequency band

constraints. The smoothed correlograms for both malaria (Fig. 4B) and rainfall (Fig. 4E) were similar to the regional synchrony, as the 95% confidence envelope contained the smoothed correlogram along the range of studied distances in each case (Fig. 4B, 4E). Similarly, as expected under a Moran effect, the regional malaria and rainfall synchrony patterns were not statistically different (Table 1). Two-month lagged rainfall had the highest positive correlation with malaria, with a decreasing association as function of increasing elevation (Fig. 5A), a pattern also observed for an analysis based only on the EMD extracted seasonal malaria IMFs (Fig. 5B). The consideration of EMD extracted interannual malaria IMFs (Fig. 5C) showed the association between interannual rainfall and interannual malaria to have a maximum positive correlation when rainfall is 1 month lagged in relation with malaria, and a maximum negative correlation when rainfall is 4 month lagged in relation with malaria, suggesting a role for rainfall temporal variability in the synchronous malaria dynamics. The SSA detrended Malaria-DMI Cross Correlation Function (Fig. 5D) showed the positive association between these time series was maximum for up to 4 months of lagged DMI at altitudes over 1600 m. When the seasonal (Fig. 5E) and interannual (Fig. 5F) malaria IMF were correlated with DMI, the association up to 4 months of lagged DMI showed to be robust at interannual scales and altitudes over 1600 m. In addition, the analysis with the IMFs also showed that DMI and seasonal components of malaria are associated at seasonal scales for 3 and 4 months of lagged DMI (Fig. 5E) and the association between DMI and malaria can be continuous along the altitudinal gradient given the emergence of significant patterns of association at altitudes below and above 1600 m (Fig. 5F). Patterns of association between malaria and DMI could be mediated by the impact of DMI on rainfall. DMI and rainfall have a correlation that decreases with altitude, which is maximized between 2 and 6 months (Fig. 6A), where DMI has nil impacts on the seasonal components of rainfall (Fig. 6B), but is positively associated with the interannual components of rainfall (Fig. 6C).

Discussion

Moran effects have seldom been observed in population dynamics [2, 3]. This could reflect the dominance of endogenous feedbacks over exogenous forcing in population dynamics [19]. For example, in diseases, a decaying synchrony with distance, or travelling waves of transmission,

have been described for both vector-borne diseases [20] and directly transmitted diseases [21]. In contrast, we found that both seasonal and interannual cycles of malaria have a non-decaying synchrony, both in 2-d distance and along an altitudinal gradient, at distances far greater than mosquito vector dispersal, which on average barely exceeds 2 km [22] or children movement in the area [23]. Moreover, the degree of synchrony in malaria time series is slightly above, yet not statistically different, from rainfall synchrony, as expected under a Moran effect [3].

A Moran effect in malaria transmission at the LVB could be explained by the monotonic dependence of *Plasmodium* parasite transmission on *Anopheles* vector density in endemic areas [4]. Mosquito population regulation is sensitive to the availability and stability of larval habitats [5, 24]. In fact, *Anopheles* vector density tracks rainfall variability in LVB in a regular fashion [12]. It takes about two months for malaria transmission to reach its peak following large rainfall events, roughly the total time of a few mosquito generations [25] including the parasite incubation period [26]. This probably implies a reactive response by mosquitoes to the transient creation of habitats by rainfall, assuming a density-dependent regulation [14], a pattern described in other species of mosquitoes vector of pathogens. Since *Anopheles* mosquitoes are ubiquitous in LVB [5, 12, 24], a synchronized amplification of their populations and malaria transmission following rainfall could explain the patterns of synchrony we report here. If this is the case, then the IOD, which has the strongest impact on rainfall at high altitudes according to climatic circulation models [8], could drive the Moran effect in malaria transmission along LVB probably by homogenizing rainfall synchrony across the altitudinal gradient, thus homogenizing weather conditions that increase mosquito productivity [24]. The existence of Moran effects in malaria transmission is a pattern that shows the non-trivial impacts of climatic variability on malaria epidemics. For example, the spatial extent of synchronous patterns in malaria transmission, i.e., the maximum distance over which malaria synchrony is constant, could be used as indicator of the minimum spatial scale for interventions aimed at eliminating malaria from a given landscape. Thus, consideration of impacts by environmental variability on malaria transmission biology is required to increase robustness in the development and implementation of malaria control and elimination programs, to at least be prepared against surprises that can arise from climatic variability, one of the many aspects shaping the complexity of malaria transmission.

References

1. Liebhold A, Koenig WD, Bjørnstad ON. Spatial synchrony in population dynamics. Annual Review of Ecology Evolution and Systematics **2004**; 35:467-490.
2. Ranta E, Lundberg P, Kaitala V. Ecology of Populations. Cambridge: Cambridge University Press, **2006**.
3. Blasius B, Stone L. Ecology: Nonlinearity and the Moran effect. Nature **2000**; 406:846-847.
4. Smith DL, Drakeley CJ, Chiyaka C, Hay SI. A quantitative analysis of transmission efficiency versus intensity for malaria. Nat Commun **2010**; 1:108.
5. Fillinger U, Sonye G, Killeen GF, Knols BGJ, Becker N. The practical importance of permanent and semipermanent habitats for controlling aquatic stages of *Anopheles gambiae sensu lato* mosquitoes: operational observations from a rural town in western Kenya. Tropical Medicine & International Health **2004**; 9:1274-1289.
6. Drakeley CJ, Carneiro I, Reyburn H, et al. Altitude-Dependent and -Independent Variations in *Plasmodium falciparum* Prevalence in Northeastern Tanzania. Journal of Infectious Diseases **2005**; 191:1589-1598.
7. Bødker R, Msangeni HA, Kisinza W, Lindsay SW. Relationship between the intensity of exposure to malaria parasites and infection in the Usambara Mountains, Tanzania. American Journal of Tropical Medicine and Hygiene **2006**; 74:716-723.
8. Anyah R, Semazzi F, Xie L. Simulated physical mechanisms associated with multi-scale climate variability over Lake Victoria Basin in East Africa. Monthly Weather Review **2006**; 134:3588-3609.
9. Hashizume M, Terao T, Minakawa N. The Indian Ocean Dipole and malaria risk in the highlands of western Kenya. Proceedings of the National Academy of Sciences of the United States of America **2009**; 106:1857-1862.
10. Behera SK, Luo J-J, Masson S, et al. Paramount impact of the Indian Ocean Dipole on the East African short rains: A CGCM Study. J Climate **2005**; 18:4514-4530.
11. Saji NH, Goswami BN, Vinayachandran PN, Yamagata T. A dipole mode in the tropical Indian Ocean. Nature **1999**; 401:360-3.
12. Minakawa N, Sonye G, Mogi M, Githeko A, Yan GY. The effects of climatic factors on the distribution and abundance of malaria vectors in Kenya. J Med Entomol **2002**; 39:833-841.
13. Shanks G, Biomndo K, Hay S, Snow R. Changing patterns of clinical malaria since 1965 among a tea estate population located in the Kenyan highlands. Transactions of the Royal Society of Tropical Medicine and Hygiene **2000**; 94:253 - 255.
14. Chaves LF, Koenraadt CJM. Climate Change and Highland Malaria: Fresh Air for a Hot Debate. The Quarterly Review of Biology **2010**; 85:27-55.
15. Shumway RH, Stoffer DS. Time series analysis and its applications. New York: Springer, **2000**.
16. Ghil M, Allen MR, Dettinger MD, et al. Advanced spectral methods for climatic time series. Reviews of Geophysics **2002**; 40.
17. Huang NE, Shen Z, Long SR, et al. The empirical mode decomposition and the Hilbert spectrum for nonlinear and non-stationary time series analysis. Proceedings of the Royal Society of London Series a-Mathematical Physical and Engineering Sciences **1998**; 454:903-995.
18. Bjørnstad ON, Falck W. Nonparametric spatial covariance functions: Estimation and testing. Environmental and Ecological Statistics **2001**; 8:53-70.
19. Turchin P. Complex population dynamics. Princeton: Princeton University Press, **2003**.
20. Cummings DAT, Irizarry RA, Huang NE, et al. Travelling waves in the occurrence of dengue haemorrhagic fever in Thailand. Nature **2004**; 427:344-347.

21. Viboud C, Bjørnstad ON, Smith DL, Simonsen L, Miller MA, Grenfell BT. Synchrony, waves, and spatial hierarchies in the spread of influenza. Science **2006**; 312:447-451.
22. Silver JB. Mosquito ecology: field sampling methods. 3rd ed. New York: Springer, **2008**.
23. Prothero RM. Migrants and Malaria. London (UK): Longmans, **1965**.
24. Minakawa N, Omukunda E, Zhou G, Githeko A, Yan G. Malaria vector productivity in relation to the highland environment in Kenya. American Journal of Tropical Medicine and Hygiene **2006**; 75:448-53.
25. Bayoh MN, Lindsay SW. Effect of temperature on the development of the aquatic stages of *Anopheles gambiae* sensu stricto (Diptera : Culicidae). Bulletin of Entomological Research **2003**; 93:375-381.
26. Lindsay SW, Birley MH. Climate change and malaria transmission. Annals of Tropical Medicine and Parasitology **1996**; 90:573-588.

Acknowledgements

We thank R. Snow for providing hospital and meteorological data for Kericho. We also thank the staff at the Kendu Bay, Maseno, Kisii and Kapsabet hospitals for their help with data compilation. LFC, MH and NM had grant support to study synchrony patterns on malaria transmission at Lake Victoria Basin. LFC is a Gaikokujin Fellow of Japan Society for the Promotion of Science.

Figure Legends

Fig. 1 Data (A) Malaria Time Series. (B) Rainfall. (C) Dipole Mode Index. (D) Trends (solid lines for Loess, dashed lines for Singular Spectrum Analysis [SSA] and dotted lines for Empirical Mode Decomposition[EMD]). There is no dashed line for Kisii and Kapsabet because the SSA was unable to detect any trends. (E) Loess detrended Malaria time series. (F) SSA detrended Malaria Time Series. (G) Malaria intrinsic mode functions, IMFs, with interannual cycles. (H) Malaria IMFs with seasonal cycles. (I) Malaria IMFs with high frequency cycles. Inset legends identify time series with colors. Color codes are shared by panels A, D, E, F, G, H, I. IMFs were derived via an EMD for each time series.

Fig. 2 Study Sites in Lake Victoria Basin, Western Kenya. Kisumu (0°6'S 34°45'E Atltitude = 1131 m); Kendu Bay (0°24’05”S, 34°39’56”E, Altitude = 1240 m); Maseno (0°00’15”S, 34°36’16”E, Altitude = 1500 m); Kisii (0°40’S, 34°46’E, Altitude = 1670 m); Kapsabet (0°12’N, 35°06’E, Altitude = 2000 m); Kericho (0°23’55”N, 35°15’30”E, Altitude = 2000 m). In the map elevation is measured in meters, m, and indicated by gray. Location color indicates the data available at each site ; blue (rainfall); green (disease) and red (disease and rainfall).

Fig. 3 Rainfall Time Series Empirical Mode Decomposition (A) Intrinsic mode functions, IMFs, with interannual cycles; (B) IMFs with seasonal cycles; (C) IMFs with high frequency cycles. Inset legends identify time series with colors.

Fig. 4 Synchrony Analysis (A) Malaria time series correlation at lag 0, r_0, as function of latitude (Lat), longitude (Long) and two-dimensional distance [2D] between the studied localities. Colors indicate the method employed to detrend the malaria time series employed to estimate r_0. (B) 2D distance spline correlogram (3 edf) for the signal obtained by adding the seasonal and interannual intrinsic mode functions from the empirical mode decomposition applied to the malaria time

series (C) Contour maps for temporal cross-correlations between the Empirical Mode Decomposition [EMD] detrended malaria time series (D) Rainfall time series correlation at lag 0, r_0, as function of latitude (Lat), longitude (Long) and 2D distance between the studied localities. (E) 2D distance spline correlogram (2 edf) for the signal obtained by adding the seasonal and interannual intrinsic mode functions from the empirical mode decomposition applied to the rainfall time series. (F) Contour maps for temporal cross-correlations among the Rainfall time series. In A, B, D, and E Synch is the estimated regional synchrony obtained with each method. In B and E dotted lines indicate the 95% confidence envelope for the smoothed correlation function, solid line, obtained with 1000 data permutations. In C and F, the y axis represents the lag for the cross correlation and the x axis represents the 2D distance. Values in the contour lines are correlations, which are significantly different from 0 when their absolute value is above 0.075 ($P<0.05$).

Fig. 5 Time scale impacts of Rainfall and Indian Ocean Dipole on malaria synchrony across an altitude gradient (A) Singular Spectrum analysis detrended malaria time series (SSA Malaria) correlation with Rainfall (B) Seasonal malaria Intrinsic Mode Function, IMF, correlation with Seasonal Rainfall IMF (C) Interannual malaria IMF correlation with Interannual Rainfall IMF (D) SSA detrended malaria correlation with Dipole mode index (DMI) (E) Seasonal malaria IMF, correlation with DMI (F) Interannual malaria IMF correlation with DMI. IMFs for each malaria time series were obtained by empirical mode decompositions. In all panels the x axis represents the lag for the cross correlation and the y axis represents the site altitude. Values in the contour lines are correlations, which are significantly different from 0 when their absolute value is above 0.075 ($P<0.05$).

Fig. 6 Time Scale association between Rainfall and Dipole mode Index (DMI). (A) Rainfall correlation with DMI (B) Seasonal rainfall Intrinsic Mode Function, IMF, correlation with DMI (C) Interannual rainfall IMF, correlation with DMI. IMFs for each malaria time series were obtained by empirical mode decompositions. The x axis represents the lag for the cross correlation and the y axis represents the site altitude. Values in the contour lines are correlations, which are significantly different from 0 when their absolute value is above 0.075 ($P<0.05$).

Figure 1

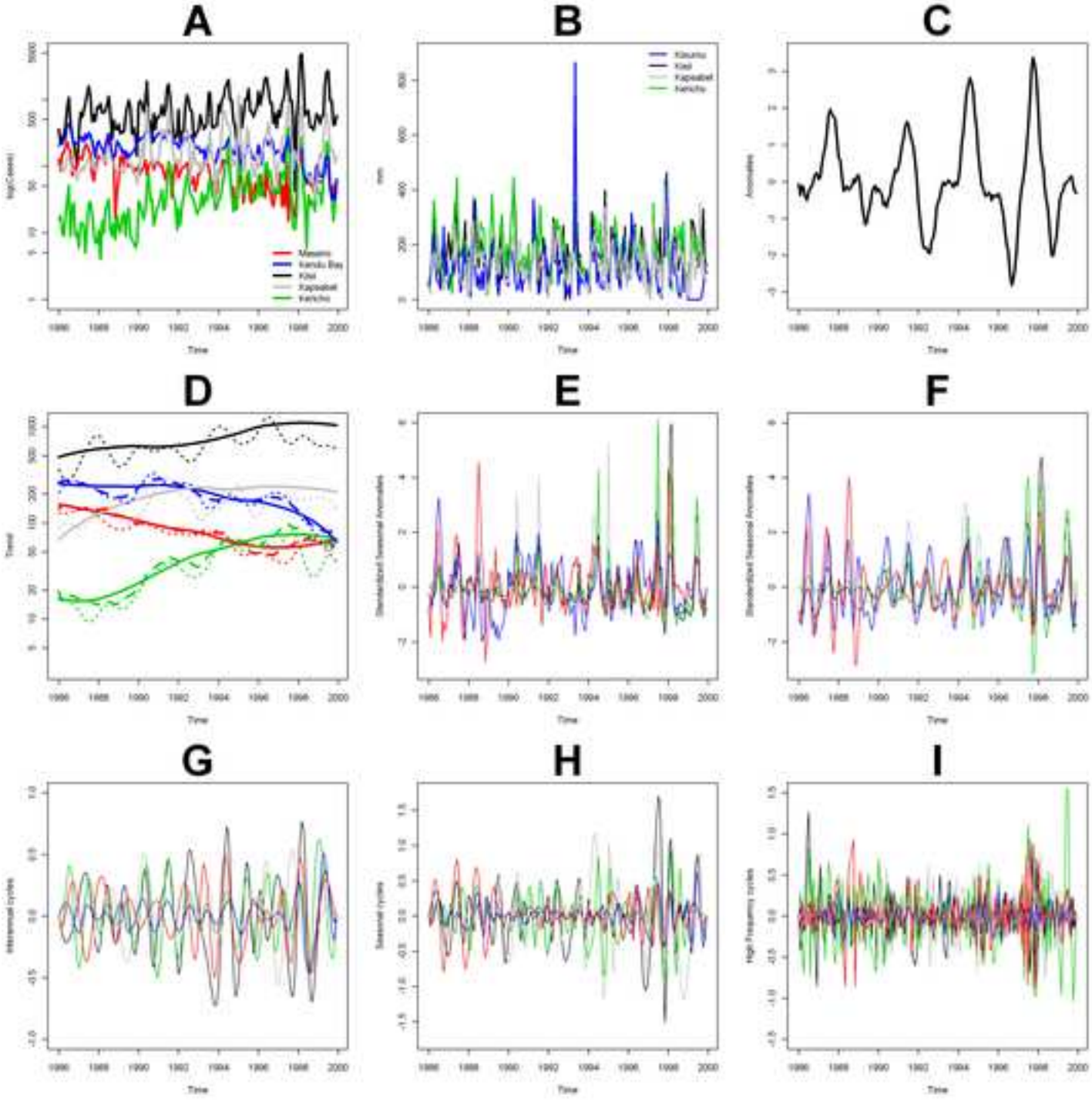


Figure 2

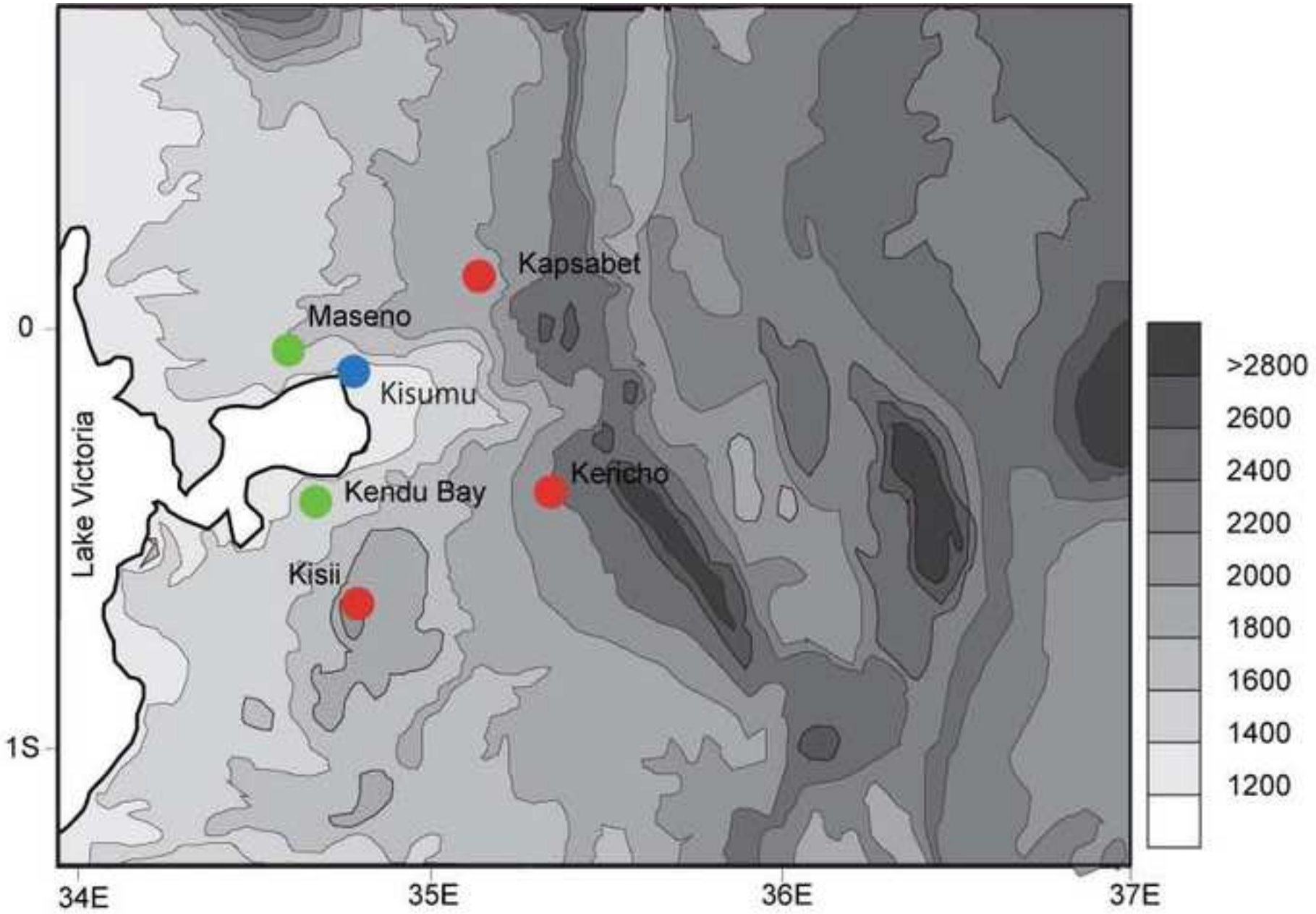

Kapsabet
Maseno
Kisumu
Kericho
Kendu Bay
Kisii
Lake Victoria
0
1S
34E
35E
36E
37E
>2800
2600
2400
2200
2000
1800
1600
1400
1200

Figure 3

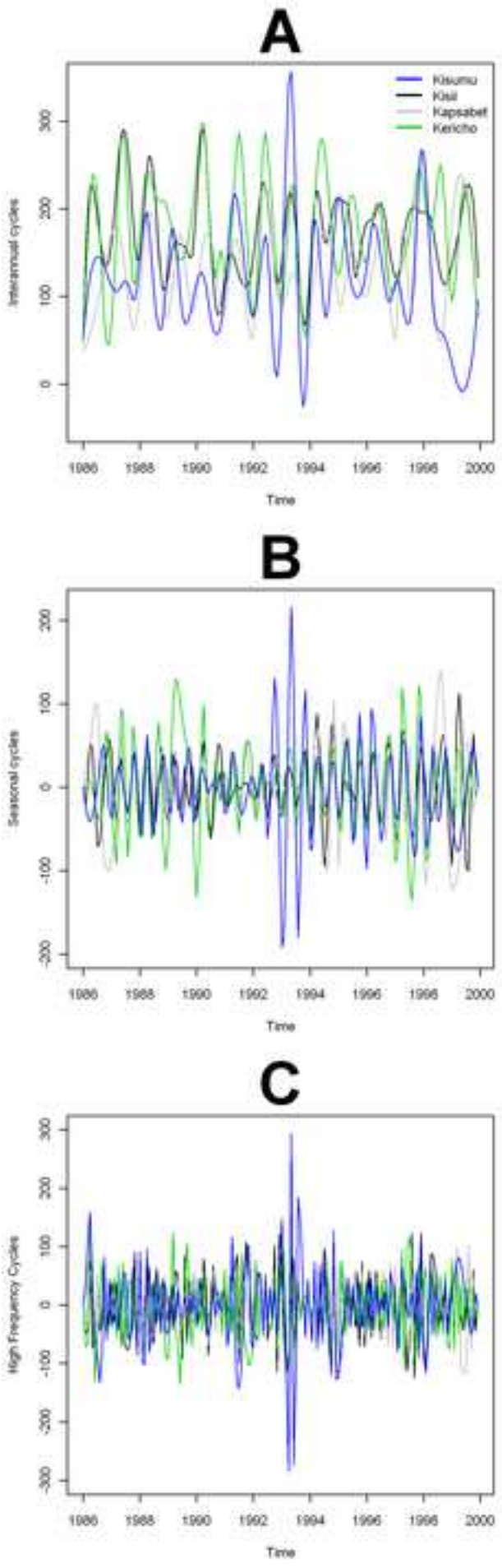

A
Kisumu
Kisii
Kapsabet
Kericho
Interannual cycles
300
200
100
0
1986
1988
1990
1992
1994
1996
1998
2000
Time
B
Seasonal cycles
200
100
0
-100
-200
1986
1988
1990
1992
1994
1996
1998
2000
Time
C
High Frequency Cycles
300
200
100
0
-100
-200
-300
1986
1988
1990
1992
1994
1996
1998
2000
Time

Figure 4

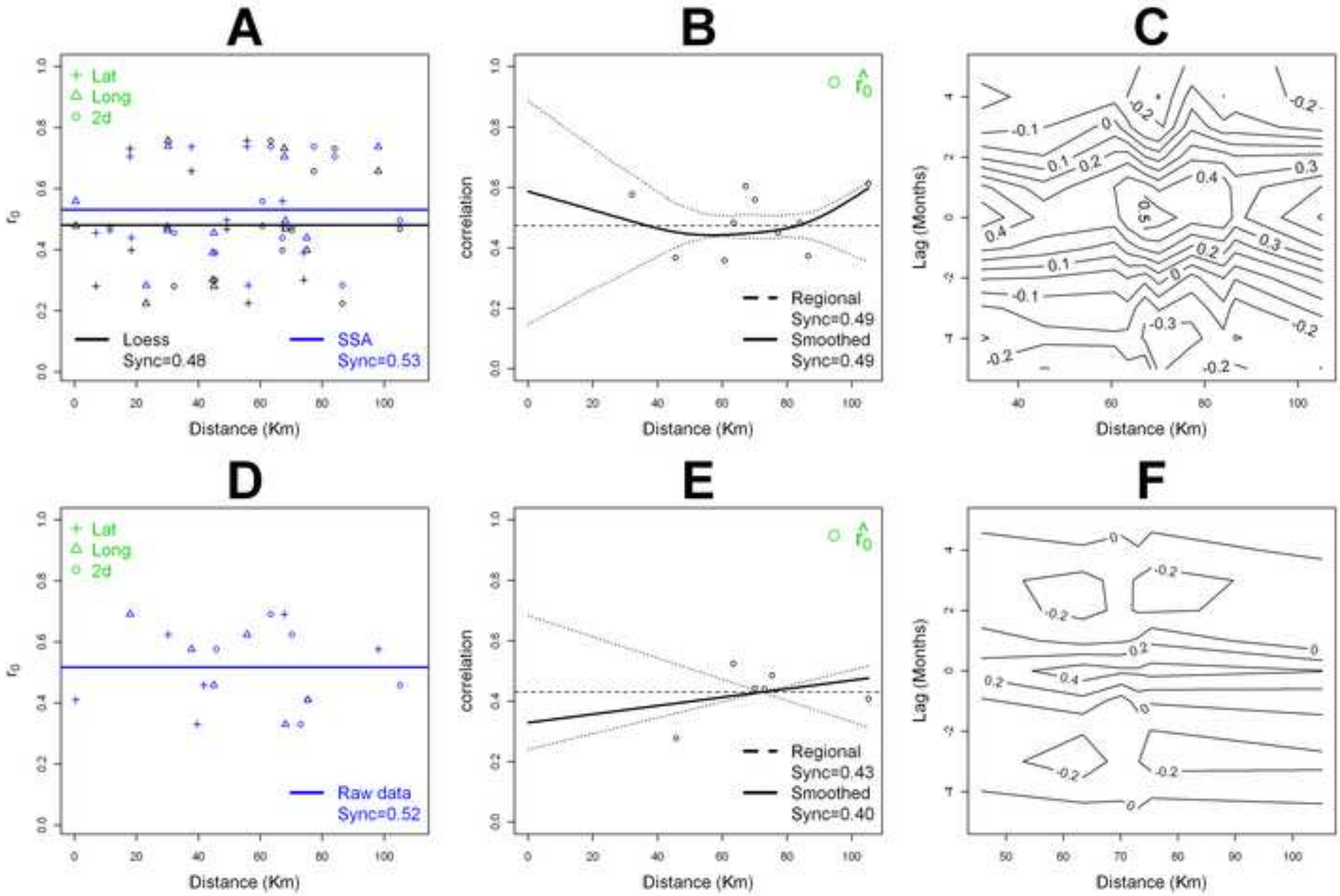

A
Lat
Long
2d
Loess
Sync=0.48
SSA
Sync=0.53
Distance (Km)
B
Regional
Sync=0.49
Smoothed
Sync=0.49
correlation
Distance (Km)
C
Lag (Months)
Distance (Km)
D
Raw data
Sync=0.52
Distance (Km)
E
Regional
Sync=0.43
Smoothed
Sync=0.40
correlation
Distance (Km)
F
Lag (Months)
Distance (Km)

Figure 5

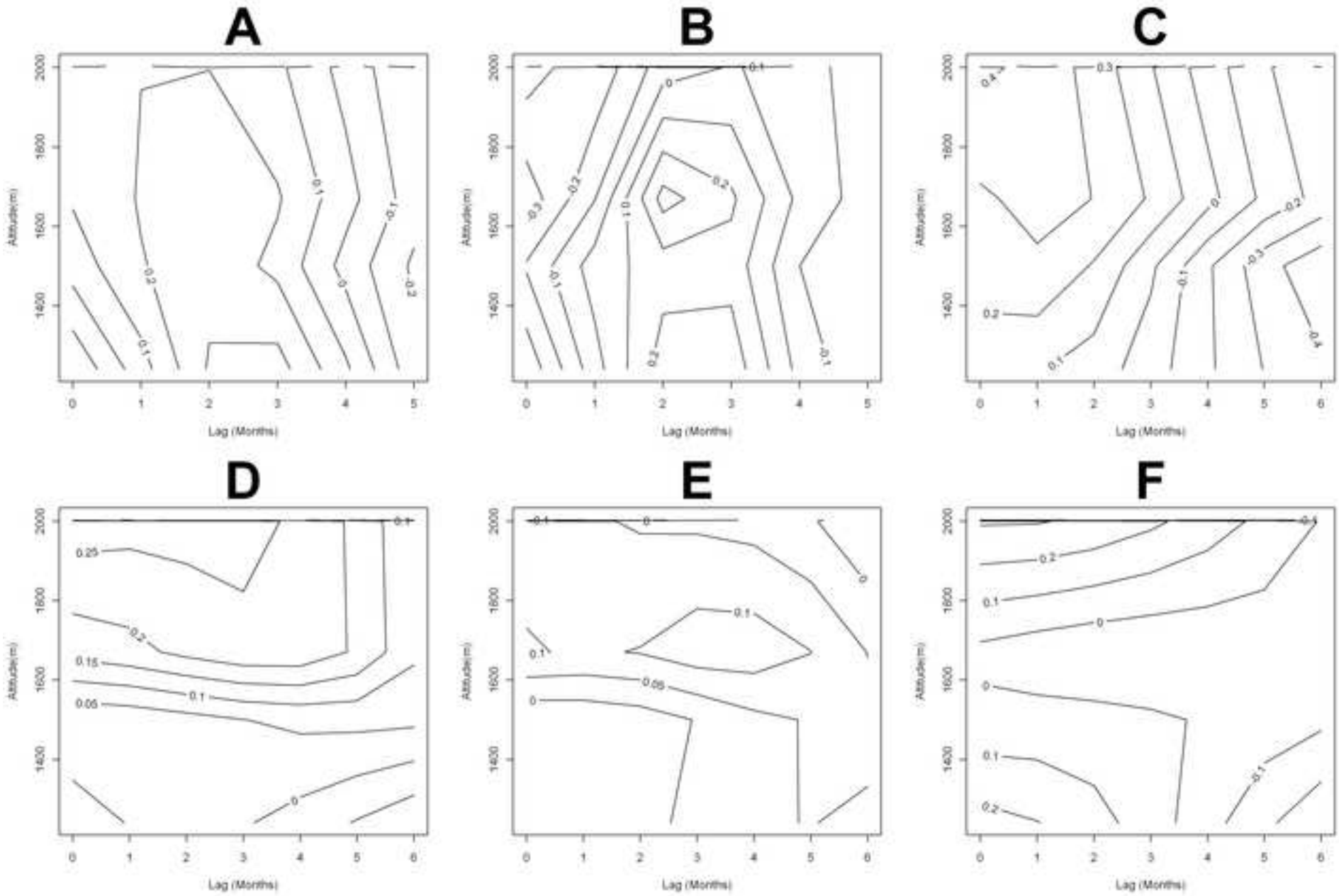


Figure 6

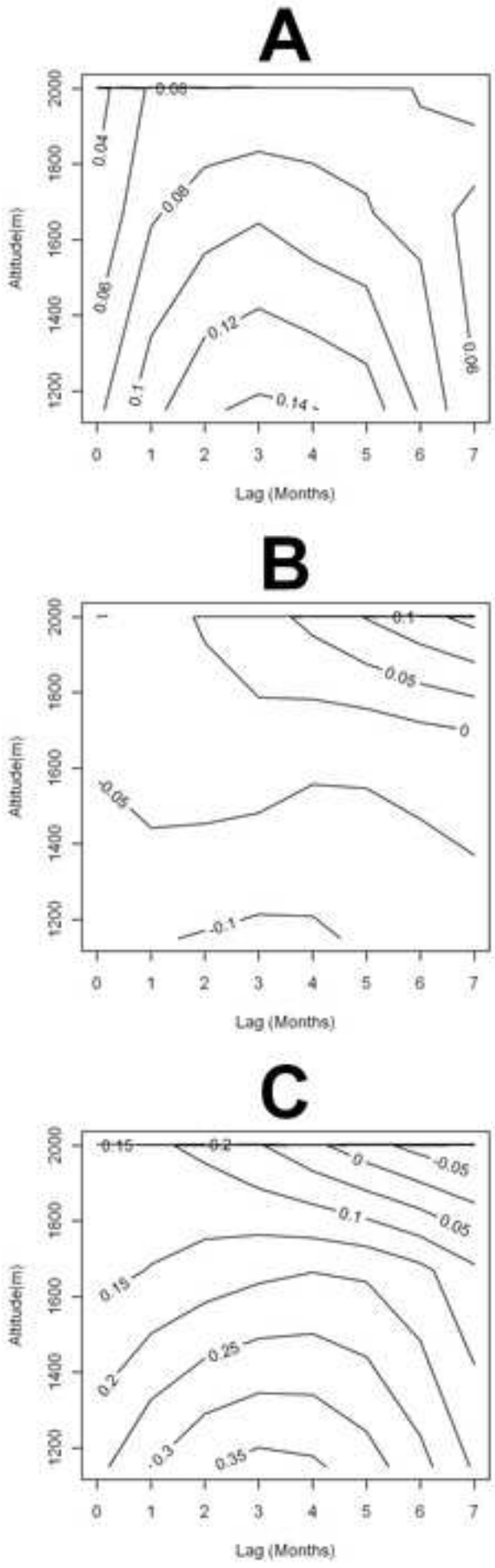

A
Altitude(m)
Lag (Months)
B
Altitude(m)
Lag (Months)
C
Altitude(m)
Lag (Months)

Table 1. Confidence limits for the regional synchrony estimates. 95% confidence limits were estimated from the standard error of maximum likelihood estimates for the regional synchrony.

Time Series	Mean ± S.E.	95% Confidence limits
Malaria-LOESS	0.48 ± 0.06	0.34 - 0.61
Malaria-SSA	0.53 ± 0.05	0.42 - 0.64
Malaria-EMD	0.49 ± 0.03	0.42 - 0.56
Rainfall-Raw Data	0.52 ± 0.06	0.37- 0.66
Rainfall-EMD	0.43 ± 0.03	0.34 - 0.51

Supplementary data

Detailed Methods

Software

All statistical analyses were performed using the statistical software R[1].

Time series detrending methods

Loess

This is a well established procedure to remove non-linear trends from time series data [2]. A non-parametric trend is fitted to the time series using local polynomials regression fits, Loess, which is then subtracted from the original series [3]. For the synchrony analysis, such residuals are then standardized to be normal and with a variance of one [2].

Singular spectrum analysis (SSA)

This non-parametric technique separates trends and oscillatory components from noise in a time series [4]. The method consists in the computation of the eigenvalues and eigenvectors from a covariance matrix [**M**] whose element m_{ij} is the covariance between lags *i* and *j*. The projection of the time series on the eigenvectors (the principal components of the matrix) reconstructs the pattern of variability associated with the selected eigenvalue, resulting in a de-noised time series [4]. The eigenvalues themselves indicate how much variance is accounted for by the different components [4] .

Empirical Mode Decomposition (EMD)

This technique decomposes time series into trends and oscillatory components. Briefly, a time series goes through an iterative sifting process which decomposes the time series into a sum of intrinsic mode functions (IMF). The algorithm to extract IMFs is as follows: (i) Envelopes are built by joining through a cubic spline all the maxima (upper envelope) and minima (lower envelope); (ii) the mean of the two envelopes is subtracted from the time series; and (iii) the

process is repeated until an IMF is obtained. IMFs should satisfy the assumption of a narrow band (which is fulfilled when the number of zero crossings and extrema are either equal or differ by one) and the mean of its upper and lower envelopes, equals zero (which renders impossible unwanted fluctuations expected by assymetric waverforms). The process of extracting IMFs can be repeated on the residuals from each IMF extraction until all cyclic components are extracted and the final residuals represent a trend for the data. Further details and a mathematically rigorous explanation are presented by Huang et al [5]. Regarding our data, we extracted three IMFs and the trend (Fig. 1D) from the malaria time series, each IMF corresponding to interannual cycles (Fig. 1G), seasonal cycles (Fig. 1H) and high frequency cycles (Fig. 1I). For the rainfall time series we only extracted two IMFs, because the extraction of a third IMF did not lead to the separation of trends, and the trends lacked any noticeable non-cyclical pattern (Fig. 3A). Like the malaria time series, the rainfall time series also had seasonal (Fig. 3B) and high frequency components (Fig. 3C). For the EMD malaria data were log-transformed, in order to minimize signal interference.

Spline Correlogram

We employed spline correlograms to study rainfall and malaria synchrony. This technique can be used to study the spatio-temporal autocorrelation among populations. Basically, smoothing splines are used to generate a functional correlogram, i.e., an assumption free and smooth function depicting spatial autocorrelation, among several time series, which depends on distance. Given the low number of time series, (5 for malaria and 4 for rainfall, numbers rendering impossible a bootstrap), we generated a null distribution from the estimator by computing spline correlograms from random time series. The random time series were constructed by sampling without replacement the detrended, and also high frequency filtered, time series, i.e., we analyzed time series without trends to ensure a stationary mean and, series without high frequency components to avoid the spurious correlations that can be expected when these components are considered. This procedure was repeated 1000 times to extract the 2.5% and 97.5 % quantiles of the null distribution, which correspond to the 95% confidence envelope of the spline correlogram [6]. For the smoothing of the 5 malaria time series we employed 3 degrees of freedom (edf), and to make a reliable comparison we used 2 edf given that we only had 4 rainfall time series.

Cross Correlation Function

Cross correlation function, CCF, is formally defined as the ratio between the cross-covariance function of two time series divided by the square root of the product of each series variance, and represents the association between time series as function of time [2].

References

1. R DCT. R: A language and environment for statistical computing
Vienna, Austria: R Foundation for Statistical Computing, **2011**.

2. Shumway RH, Stoffer DS. Time series analysis and its applications. New York: Springer, **2000**.

3. Ranta E, Lundberg P, Kaitala V. Ecology of Populations. Cambridge: Cambridge University Press, **2006**.

4. Ghil M, Allen MR, Dettinger MD, et al. Advanced spectral methods for climatic time series. Reviews of Geophysics **2002**; 40.

5. Huang NE, Shen Z, Long SR, et al. The empirical mode decomposition and the Hilbert spectrum for nonlinear and non-stationary time series analysis. Proceedings of the Royal Society of London Series a-Mathematical Physical and Engineering Sciences **1998**; 454:903-995.

6. Bjørnstad ON, Falck W. Nonparametric spatial covariance functions: Estimation and testing. Environmental and Ecological Statistics **2001**; 8:53-70.